




Solid state diffusion and reactivity in the multiferroic $\text{BiFeO}_3\text{-Bi}_4\text{Ti}_3\text{O}_{12}$ composite system

Carlos Gumiel¹, Mara S. Bernardo¹, Pablo G. Villanueva², Teresa Jardiel², Jose De Frutos¹, Amador C. Caballero², and Marco Peiteado^{1,*} 

¹POEMMA-CEMDATIC, ETSI Telecomunicación (UPM), Universidad Politécnica de Madrid, Avda Complutense 30, 28040 Madrid, Spain

²Department of Electroceramics, Instituto de Cerámica y Vidrio (CSIC), Kelsen 5, 28049 Madrid, Spain

Received: 20 September 2016

Accepted: 8 December 2016

Published online:

20 December 2016

© Springer Science+Business Media New York 2016

ABSTRACT

In the search of multiferroic materials with enhanced magnetoelectric response, the $\text{BiFeO}_3\text{-Bi}_4\text{Ti}_3\text{O}_{12}$ composite system has been proposed as a promising candidate. However, in order to ensure an effective coupling between the antiferromagnetic and the ferroelectric-order parameters, a high structural quality of the oxide heterostructure (well-matched interface) must be attained. This implies the absence of any inter-diffusion process across the interface during the consolidation of the composite assembly. In this contribution, we have analysed the different diffusion scenarios that could be established in this nominal $\text{BiFeO}_3\text{-Bi}_4\text{Ti}_3\text{O}_{12}$ system as a function of the specific reactivity of the involved compounds. The obtained results clearly identify how and when that diffusion is produced, so now it can be controlled to ensure the maximum exploitation of the potential multiferroic properties of this candidate system.

Introduction

A case system in the search for novel materials with enhanced functionality is that of multiferroic oxides, in particular those showing magnetoelectric effect. Magnetoelectric multiferroics are compounds displaying concurrent and coupled magnetic polar order, and in the best scenario these orders are ferromagnetism and ferroelectricity [1, 2]. Nowadays, single-phase oxide systems can be prepared in which an intrinsic multiple ferroic order is allowed based on symmetry arguments [3–6]. However, constraint considerations associated with the simultaneous

presence of magnetism and ferroelectricity typically lead to low critical temperatures in those single-phase structures, making their multiferroic response unpractical. Such limitations have redirected efforts to a more realistic approach, which is the fabrication of heterogeneous composite systems [7–11]. In the composite arrangement, the different order parameters need not coexist in the same phase, while the symmetry rupture ensued from the different symmetries of the heterostructure would originate an extrinsic coupling at the interface; particularly, nanostructured composites with large surface area such as concentric core-shell particulates or

Address correspondence to E-mail: marco.peiteado@upm.es

multilayer film arrays can result especially effective [12–15]. In this search, different composite formulations have been considered and one especially promising is that constituted by the $\text{BiFeO}_3\text{--Bi}_4\text{Ti}_3\text{O}_{12}$ binary system. BiFeO_3 (BFO) is itself a multiferroic single-phase material which shows ferroelectric ordering with high Curie temperature $T_C = 1103$ K and G-type antiferromagnetic ordering with a relatively high Néel temperature $T_N = 634$ K [3, 16]; however it exhibits a small polarization (much smaller than the one theoretically predicted) and this is attributed to a high leakage current. $\text{Bi}_4\text{Ti}_3\text{O}_{12}$ (BiT) on the other hand is a well-known ferroelectric material, although with strong anisotropic electric properties [17, 18]. Despite these individual drawbacks, the combination of both oxides into a selected and properly doped configuration is expected to yield a composite material in which the coexistence of antiferromagnetic and ferroelectric-order parameters can be attained with a substantially reduction of the leakage current [19–21]. Furthermore, leaning on the similitudes of the involved crystal structures (both oxides comprising perovskite-like constituent units), a well-matched interface could be also presumed, hence enabling an effective coupling between the electric and magnetic properties [22–25]. However before going into a detailed analysis of the specific processing conditions and/or the potential multiferroic properties of the $\text{BiFeO}_3\text{--Bi}_4\text{Ti}_3\text{O}_{12}$ composite system, there is one critical issue which shall be considered: in order to ensure a high structural quality (i.e. a well-matched interface) of the oxide heterostructure, no diffusion processes between the two involved phases should be produced and, if produced, they should be controlled and/or blocked. Usually the energy provided during the consolidation stage of the composite configuration induces the establishment of diffusion paths across the interface; from the point of view of the multiferroic response, this can result to be very detrimental: an excessive or uncontrolled diffusion not only spoils the functional properties of each particular phase but it could also transform the interface (e.g. by forming a new phase), eventually ruining the extrinsic coupling between the two ferroic phases. Accordingly, a detailed analysis of the solid state reactivity and the diffusion trends of the $\text{BiFeO}_3\text{--Bi}_4\text{Ti}_3\text{O}_{12}$ composite system could be very helpful to ensure the maximum exploitation of its multiferroic potential. In this view, the research here presented pursues to identify all the possible diffusion scenarios that could be found when

preparing/building the composite assembly (whatever it may be). This implies different configurations and also starting scenarios of different reactivities because, eventually, the magnitude of the diffusion processes will be as well defined by the specific reactivity of the starting powders. Particularly, we have achieved this goal by using the well-known technique of the diffusion couples. This technique has been proved quite successful for studying the interaction between different binary, ternary and multiphase ceramic systems [26–28]. On using it, we are taking into account that when reactants are not in direct contact, the reaction is entirely dependent on the diffusion of reactants [29, 30].

Materials and methods

As introduced, the solid state reactivity of the BFO–BiT composite system was analysed using the diffusion couples methodology. This technique consists in bringing together two pellets, one of each particular material, to then follow the structural and compositional evolution across the outlined interface as a function of temperature. Such evolution is monitored in terms of dissimilar cations diffusing into the opposite pellets, either forming solid solutions or new phases; in this work, this means titanium species diffusing into the BFO pellet and iron species diffusing into the BiT counterpart. To run all these analyses, three different sets of experiments were indeed performed. They mainly differed on the specific composition and reactivity of the green powders constituting the pellets of the couple. In a first set of experiments, powders of already synthesized BiFeO_3 and $\text{Bi}_4\text{Ti}_3\text{O}_{12}$ nominal compounds were employed; both were prepared following a conventional solid state procedure, involving an ultimate thermal treatment at $800\text{ }^\circ\text{C}/2$ h for the BiFeO_3 powder [31] and $800\text{ }^\circ\text{C}/4$ h for the $\text{Bi}_4\text{Ti}_3\text{O}_{12}$ one [32]. Once synthesized, these two powders were attrition-milled (2 h in ethanol media) prior to the formation of the couples; in both cases, a monomodal particle size distribution was obtained as measured on a laser diffraction particle size analyser (Malvern Mastersizer), with a $D(v,0.5)$ of $3.0\text{ }\mu\text{m}$ for the BiFeO_3 powder and $1.5\text{ }\mu\text{m}$ for the $\text{Bi}_4\text{Ti}_3\text{O}_{12}$ powder. In the second group of experiments the pellets were composed by the stoichiometric mixture of the corresponding raw oxide precursors: Bi_2O_3 and Fe_2O_3 for

the BFO pellet and Bi_2O_3 and TiO_2 for the BiT counterpart. In this case, the raw oxide powders were simply attrition-milled (2 h in ethanol media) so to provide a similar particle size that facilitates an intimate mixture. The corresponding $D(v, 0.5)$ were $1.2 \mu\text{m}$ for the $\text{Bi}_2\text{O}_3 + \text{Fe}_2\text{O}_3$ mixture and $1.6 \mu\text{m}$ for the $\text{Bi}_2\text{O}_3 + \text{TiO}_2$ mixture, both again exhibiting a monomodal distribution. Finally, a third series of couples was evaluated in which the starting powders composing the pellets were obtained via co-precipitation. On one hand, $\text{Bi}(\text{NO}_3)_3 \cdot 5\text{H}_2\text{O}$ and $\text{Fe}(\text{NO}_3)_3 \cdot 9\text{H}_2\text{O}$ were used as precursors of the nominal BFO-precipitated composition. Both nitrates were dissolved in concentrated nitric acid and a solid precipitate was produced after dripping an aqueous solution of NH_4OH (50 vol%) [28]. The as-obtained precipitate was filtrated, calcined at $300 \text{ }^\circ\text{C}$ for 30 min and finally attrition-milled to yield a homogenous powder with an average particle size around 100 nm, as measured on the SEM microscope (FESEM Hitachi S-4700). On the other hand, the BiT nominal precipitate was obtained from mixing the Bi^{3+} solution ($\text{Bi}(\text{NO}_3)_3 \cdot 5\text{H}_2\text{O}$ dissolved in HNO_3) and titanium(IV) tert-butoxide, $\text{Ti}[\text{OC}(\text{CH}_3)_3]_4$ in ethanol media, again using ammonium hydroxide to generate the solid powder [32]. This precipitate was filtrated and calcined at $300 \text{ }^\circ\text{C}$ for 30 min, and after the corresponding milling step a homogenous powder was again obtained this time averaging a particle size of 50 nm. Table 1 summarizes the differences between the three couples series used to analyse the diffusion trends of the BFO–BiT composite system (reagent-grade raw materials from Sigma-Aldrich were used for all experiments).

The couples were all prepared following a typical procedure as described elsewhere [33]: a 20-mm

diameter base of the BFO powder composition was first pressed at 50 MPa. Subsequently, a 6-mm diameter pellet of the BiT powder previously pressed at 200 MPa was placed over this base, and the die was then filled with more BFO powder until the BiT pellet is plenty covered. Eventually the whole ensemble was pressed at 250 MPa. Figure 1 illustrates a scheme of the prepared couples; notice that the selection of BiT as the inside pellet is arbitrary. The as-prepared couples were heated at temperatures ranging from 650 to $750 \text{ }^\circ\text{C}$, applying in all cases a prolonged dwell time of 20 h that may allow a widespread diffusion (when produced). Three samples were fired at each temperature. Thermal treatments below $650 \text{ }^\circ\text{C}$ generally seemed too low to provoke diffusion. On the other hand, $750 \text{ }^\circ\text{C}$ represented a kind of upper limit, since higher temperatures would be excessively close to the melting point of some of the implied Bi-rich phases. In this contribution, only the experiments showing the most significant results will be disclosed.

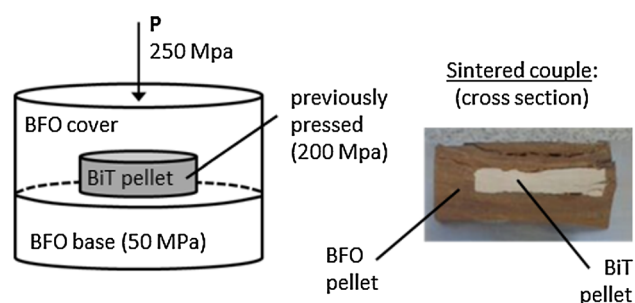


Figure 1 Preparation of the nominal BiT–BFO diffusion couples. Upon heating, the sample is embedded in resin and cut on its half for the subsequent characterization (image on the right).

Table 1 Nominal composition of the starting powders used to prepare the three sets of diffusion couples analysed in this work

	Nominal composition of the starting powders	
	BFO counterpart pellet	BiT counterpart pellet
Couples series 1 Solid state synthesized compounds	BiFeO_3	$\text{Bi}_4\text{Ti}_3\text{O}_{12}$
Couples series 2 Mixed oxides	$\text{Bi}_2\text{O}_3 + \text{Fe}_2\text{O}_3$	$\text{Bi}_2\text{O}_3 + \text{TiO}_2$
Couples series 3 Co-precipitated precursors	Solid precipitated from Bi(III) and Fe(III) precursors	Solid precipitated from Bi(III) and Ti(IV) precursors

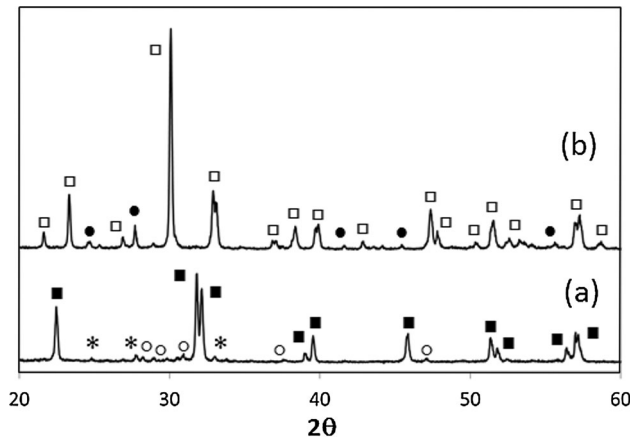


Figure 2 XRD patterns of *a* BiFeO₃ and *b* Bi₄Ti₃O₁₂ as-prepared compounds that were used in the first couples series. Filled square BiFeO₃, asterisk Bi₂₅FeO₃₉, open circle Bi₂Fe₄O₉, open square Bi₄Ti₃O₁₂, filled circle Bi₁₂TiO₂₀.

Particle size characterization was done by X-ray diffraction (XRD) and field emission scanning electron microscopy equipped with energy dispersive X-ray spectroscopy analysis (FESEM–EDS). For the XRD, characterization step-scanned patterns were collected using CuK α 1 radiation on a Bruker AXS D8 Advance diffractometer with a LynxEye 1-D linear detector and a secondary monochromator (Karlsruhe, Germany). As it will be described throughout the article, XRD is mainly used to investigate the composition of the different starting powders constituting the couples; notice that in these samples polishing is to be avoided so to keep the local composition unaltered, and this eventually restrains the use of XRD to characterize the interfaces. The FESEM–EDS analyses were performed on Cold FESEM Hitachi S-4700 microscope (Tokyo, Japan); in all cases, up to 15

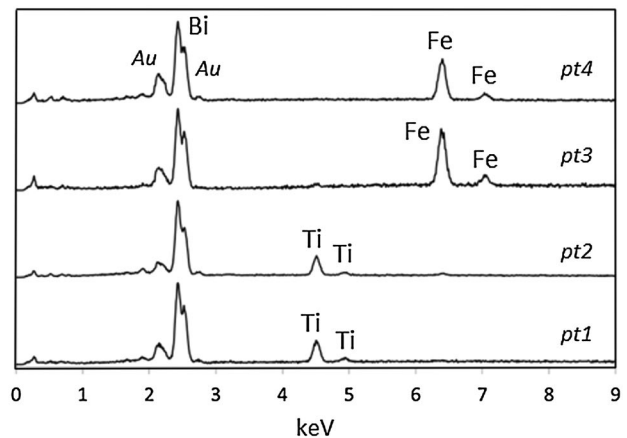
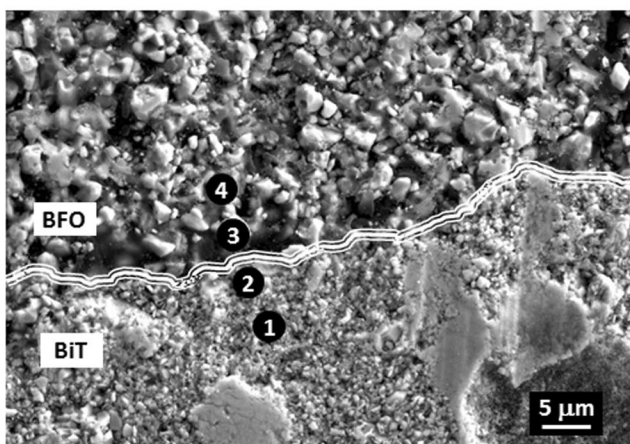
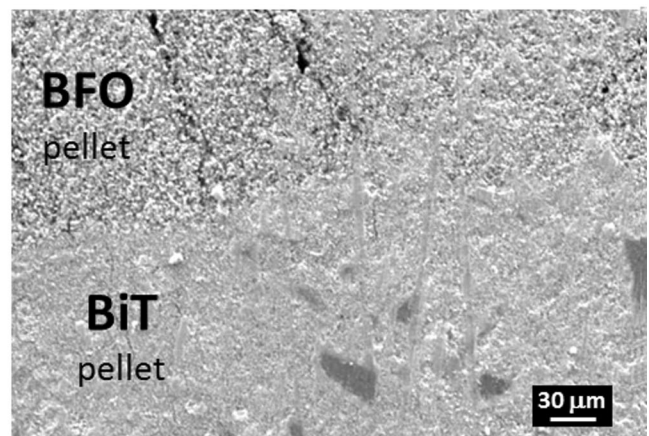
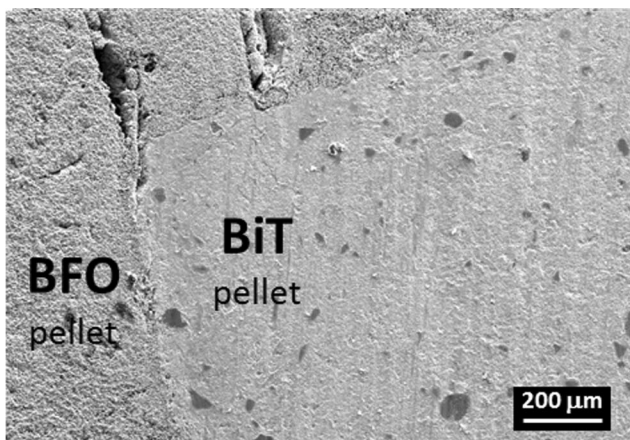


Figure 3 FESEM–EDS analyses corresponding to one sample of the first couples series heated at 750 °C/20 h. No sign of titanium is ever detected inside the BFO pellet, and equally no trace of iron seems to diffuse into the BiT counterpart.

different EDS spectra were collected in equivalent locations/distances in order to attain representative results.

Results and discussion

The first series of diffusion couples comprised the use of already synthesized BiFeO_3 and $\text{Bi}_4\text{Ti}_3\text{O}_{12}$ nominal compounds as the constituent powders of the pellets. Figure 2 shows the corresponding XRD patterns for such powders obtained via a conventional solid state procedure. As expected, rhombohedral BiFeO_3 (ICDD file no. 071-2494) and tetragonal $\text{Bi}_4\text{Ti}_3\text{O}_{12}$ (ICDD file no. 035-0795) are the major phases in the respective compositions, but the presence of secondary phases is also evidenced in both materials. The obtaining of single-phase compounds is not an easy task (particularly in the case of BiFeO_3 [28]), so we continued the analyses assuming also that the minority presence of the secondary phases does not significantly affect the overall diffusion trends.

Figure 3 shows different FESEM images of the couple after the thermal treatment at $750\text{ }^\circ\text{C}/20\text{ h}$, the interface between both pellets being highlighted to facilitate comprehension. EDS analyses evidenced no diffusion in both directions, neither of titanium into the BFO pellet nor of iron into the BiT counterpart. Figure 3 also shows some selected EDS measurements which illustrate the lack of diffusion at both sides of the couple. Essentially these first results indicate that once the two oxides are constituted, no further inter-diffusion processes may spoil the formation of the specific composite configuration (i.e. core-shell units or layered films).

In a second set of experiments, the couples were raised starting not from the already formed double oxides but from the corresponding mixture of raw oxide precursors, i.e. from $\text{Bi}_2\text{O}_3 + \text{Fe}_2\text{O}_3$ for the BFO pellet and from $\text{Bi}_2\text{O}_3 + \text{TiO}_2$ for the BiT pellet (Table 1). In a sense, this represents not only a more realistic scenario for a solid state conventional processing but it also implies a change in reactivity, an increase actually, which may affect the diffusion charts. With this in mind, the corresponding couples were prepared, but initially no clear results could be obtained for any of the thermal treatments that were tested. As a matter of fact, the presence of one same reactant in the two pellets of the couple, i.e. Bi_2O_3 , largely hampers the formation of a well-defined

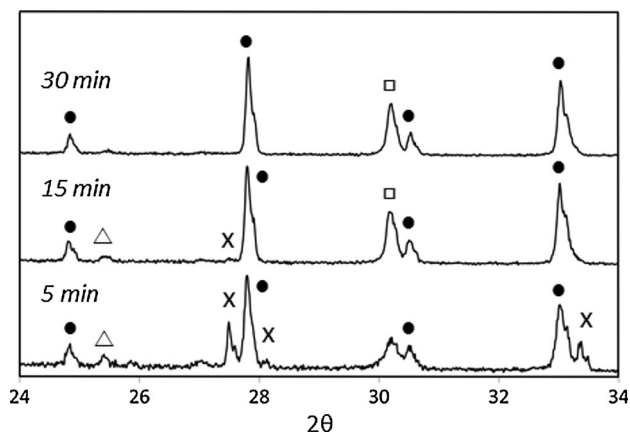


Figure 4 XRD patterns of the BiT inside pellets used in the second couples series after being subjected to 5, 15 and 30 min of pre-curing treatment at $700\text{ }^\circ\text{C}$. Open square $\text{Bi}_4\text{Ti}_3\text{O}_{12}$, filled circle $\text{Bi}_{12}\text{TiO}_{20}$, cross Bi_2O_3 , open triangle TiO_2 .

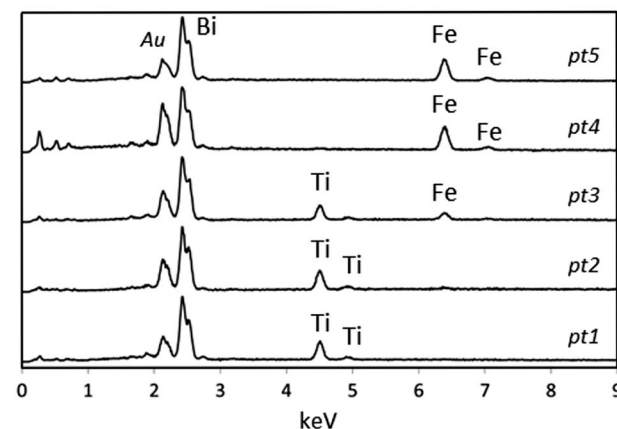
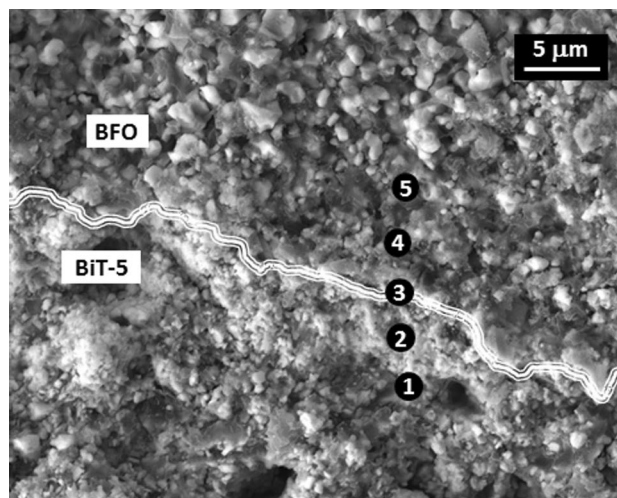


Figure 5 FESEM–EDS analyses corresponding to the couple of the second series prepared with the 5 min-cured BiT pellet and heated at $750\text{ }^\circ\text{C}/20\text{ h}$. Again no trace diffusion can be detected at both sides of the interface.

interface region below 10–15 microns and, eventually, this makes unreliable the diffusion analyses by EDS. To overcome this problem, we operated as follows: prior to the conformation of the couple, the inside pellet was subjected to a fast-firing curing process, introducing the pellet on a previously heated furnace for a few minutes and rapidly quenching it to room temperature. In doing so, the two confronted pellets preserve certain individuality in the couple, up to a very thin interface, but at the same time an inter-diffusion process between them could be still produced. Specifically, the inside BiT pellets were subjected to 5, 15 and 30 min of curing treatment at 700 °C. These precise conditions were initially settled not to produce a very large amount of crystallized $\text{Bi}_4\text{Ti}_3\text{O}_{12}$ at the surface of the pellet, otherwise we may have a similar scenario to that already analysed in the first couple series. Figure 4 depicts the corresponding XRD patterns as taken from the surface of the cured pellets. Notice that for the aim of comparison, the collected diffractograms were all normalized to the peak of maximum intensity. As can be seen, the 5 min firing at 700 °C is enough to produce the first traces of $\text{Bi}_4\text{Ti}_3\text{O}_{12}$ plus a notorious amount of the intermediate $\text{Bi}_{12}\text{TiO}_{20}$ sillenite phase, although a certain volume of unreacted Bi_2O_3 and TiO_2 is still detected; when the pellet is cured for 15 min or longer the presence of these two reactants gradually vanishes (to the XRD eye) at the expense of more $\text{Bi}_4\text{Ti}_3\text{O}_{12}$, the amount of sillenite also diminishing proportionally.

With these cured pellets new couples were assembled and fired, and now in all cases a well-defined interface was perceived which allowed the corresponding diffusion analyses. Figure 5 shows the FESEM–EDS measurements performed on the couple produced with the 5 min-cured BiT pellet, and heated at 750 °C for 20 h. No titanium was ever detected inside the BFO pellet and similarly no trace of iron could be ever identified inside the BiT counterpart. Necessarily this same result applies for the experiments conducted with the BiT pellets cured for longer times (not shown here) and suggests that from the point of view of solid state diffusion both TiO_2 and Fe_2O_3 also behave as inert specimens: the two oxides just react at certain temperature with surrounding Bi_2O_3 to form the corresponding BiT and BFO compounds, respectively, but during the whole heating stage no titanium or iron species are neatly released from the respective anatase and corundum structures to freely diffuse through the couple.

Indeed such poor disposition of Fe_2O_3 to diffuse from the BFO structure was already reported [28]; now the same lack of reactivity for TiO_2 is observed.

As indicated in the experimental section, a third series of couples was attempted in which the starting powders were obtained via co-precipitation. This is certainly a much more reactive setup and, for example, it resembles that of a multilayer composite configuration processed by a standard sol-gel methodology. The XRD patterns of these two precipitated powders are shown in Fig. 6; in both cases, the sizeable width of the spotted peaks together with a low signal-to-noise ratio shall be taken as an evidence of increased reactivity. Following our previous routine, the BiT inside pellet was again subjected to a fast-firing step of 5, 15 and 30 min prior to the configuration of the couple. Moreover, anticipating a higher diffusivity in these couples, one BiT pellet was also pre-cured for 60 min. The resultant XRD patterns are all depicted in Fig. 7 and as observed, the presence of the $\text{Bi}_4\text{Ti}_3\text{O}_{12}$ phase is now prominent in all these fired samples (strong difference with the BiT pre-cured pellets prepared from the raw oxides, see Fig. 4). The couples were subsequently prepared using these pre-cured pellets and Fig. 8 specifically shows the characterization performed on the samples heated at 700 °C/20 h (the higher reactivity of the powders yielded best results at lower temperatures). As depicted, no movement of Ti species across the interface is again detected, but this time a short-range diffusion of Fe into the opposed BiT pellet is observed. Furthermore, this iron flow is barely

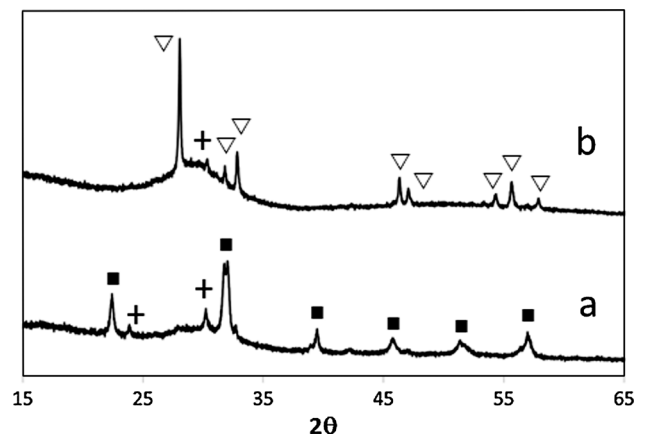


Figure 6 XRD patterns of nominal *a* BFO and *b* BiT co-precipitated (and 300 °C calcined) powders, that were used in the third couples series. Filled square BiFeO_3 , plus $\text{Bi}(\text{OH})_3$, inverted open triangle $\beta\text{-Bi}_2\text{O}_3$.

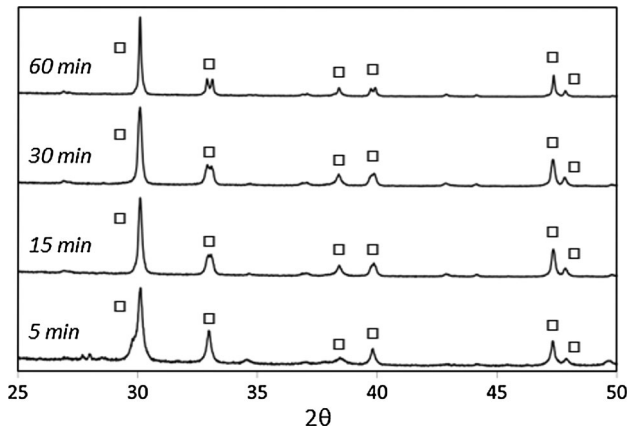


Figure 7 XRD patterns of the BiT inside pellets used in the third couples series after being subjected to 5, 15, 30 and 60 min of pre-curing treatment at 700 °C (open square $\text{Bi}_4\text{Ti}_3\text{O}_{12}$).

attenuated even after curing the BiT pellet for 1 h. Clearly, this different behaviour must be attributed to the higher reactivity of the starting BFO

precipitate. By higher reactivity, we want to denote that the starting powder needs a smaller amount of energy to activate all the solid state diffusion and mass transport processes in the system. As a matter of fact, diffusion is one of many processes that are characterized by an energy barrier between the initial and final states [34] and, for given conditions of pressure and temperature, the chemical reactivity of the starting powders can become a determining factor. Likewise, for good chemical reactivity a fine particle size is desirable; in this sense, we can consider that the nanometric size of the precipitated BFO particles make them more reactive than, for example, the solid state pre-formed BiFeO_3 powder in couple series 1. This higher reactivity also accounts for faster diffusion rates, eventually allowing the diffusion of iron into the BiT pellet to a point that not even the formation of a well-crystallized $\text{Bi}_4\text{Ti}_3\text{O}_{12}$ can impede it and/or stop it. On the contrary the titanium species, now trapped in such

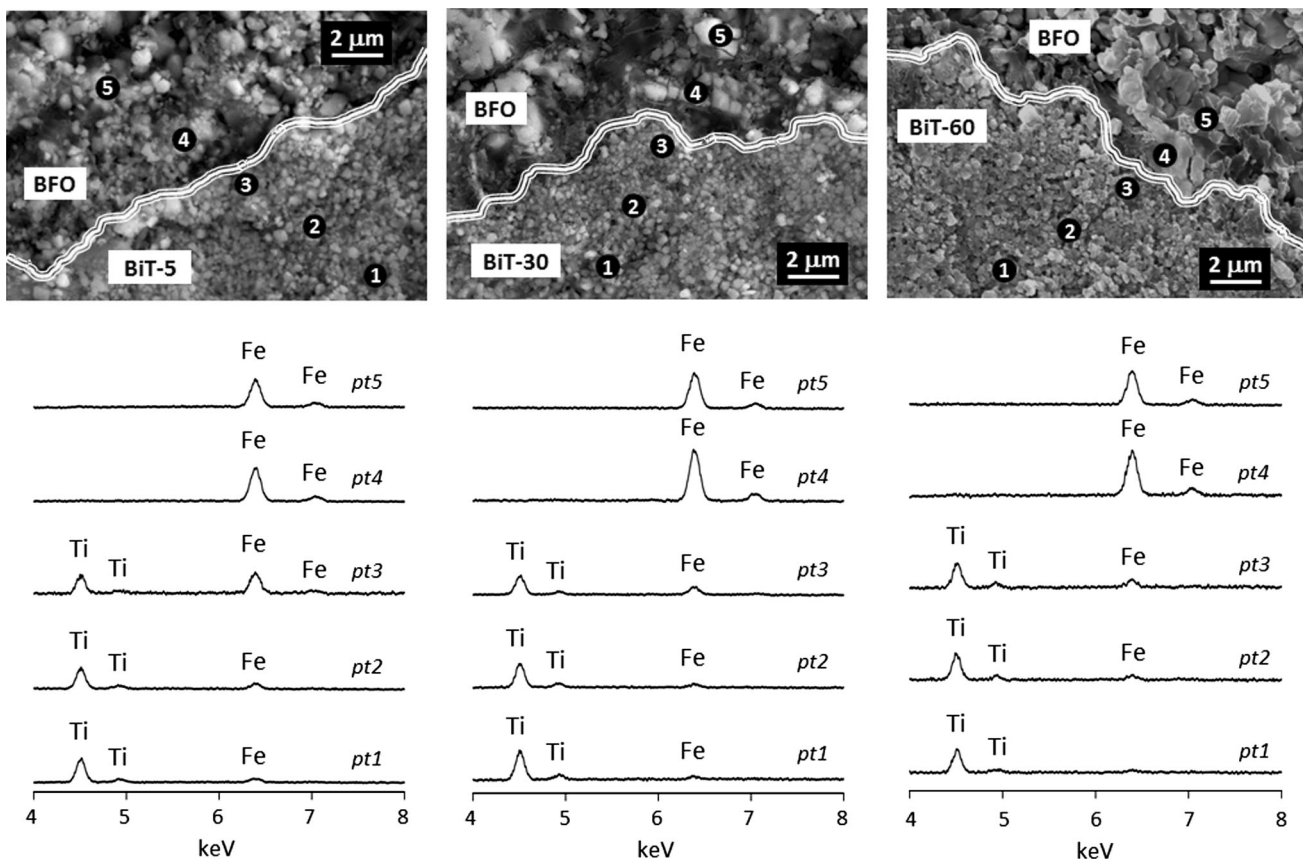


Figure 8 FESEM–EDS analyses of the third couples series: samples prepared with BiT pellets previously cured during 5 min (left), 30 min (middle) and 1 h (right) and heated at 700 °C/20 h. Now a short-range diffusion is initially observed in both sides of

the interface. In the case of Ti, the process seems to be stopped after curing the BiT pellet for 30 min or longer, whereas the diffusion of Fe is barely attenuated even after 1 h of curing treatment.

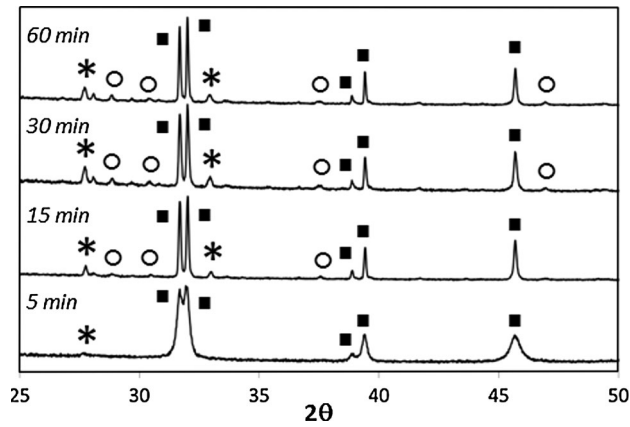


Figure 9 XRD patterns of the BFO pre-cured pellets used in the inverse configuration of the third couples series. Filled square BiFeO_3 , asterisk $\text{Bi}_{25}\text{Fe}_4\text{O}_{39}$, open circle $\text{Bi}_2\text{Fe}_4\text{O}_9$.

$\text{Bi}_4\text{Ti}_3\text{O}_{12}$ Aurivillius pre-formed structure, still remain inactive to diffusion.

Following these results, a last set of experiments was conducted to complete our diffusion analyses. As we stated in the experimental section, the specific configuration of the couples with the BiT pellets always placed inside was initially arbitrary. However, considering the pre-curing step required to (partially) disengage the involved interfaces, this may not be irrelevant. Accordingly, working with these last co-precipitated powders we prepared some “inverted couples”, placing BFO pre-cured pellets inside and leaving the BiT pellets outside. Figure 9 first shows the XRD patterns of the BFO-precipitated pellets after the corresponding 5, 15, 30 and 60 min of fast-firing at 700 °C; as depicted the pre-curing treatment is enough to produce a major amount of BiFeO_3 phase in all cases. Figure 10 then shows the FESEM characterization performed on the couple prepared with the BFO pellet pre-cured for 15 min. We chose this one as representative but the fact is that all the “inverted couples” led to the same clear result: no diffusion is detected in any direction, neither of Ti into the BFO pellet nor of Fe into the BiT counterpart. These results should be interpreted as follows: on one hand Titanium ions would now diffuse from a much more reactive situation, the as-precipitated precursor; however, this increased reactivity better leads to a quick formation of the $\text{Bi}_4\text{Ti}_3\text{O}_{12}$ compound and this eventually impedes any free titanium to diffuse into the other side of the couple. On the other hand, the absence of Fe diffusion is consistent with what we observed in the first series of couples: once the BiFeO_3

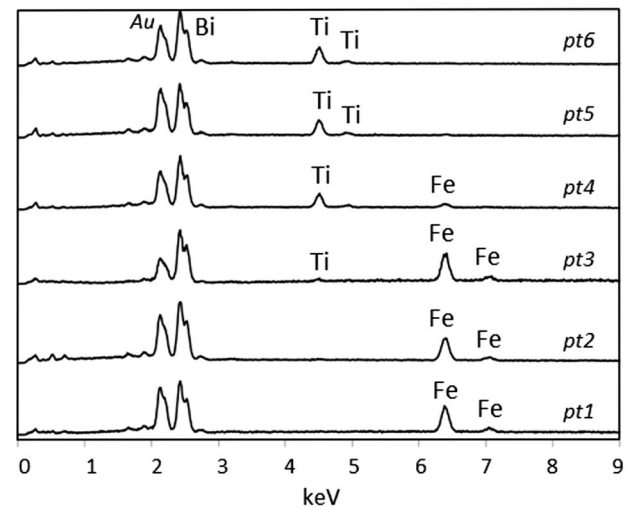
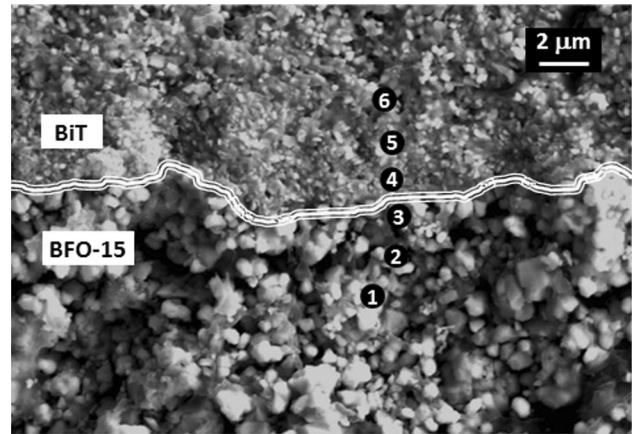


Figure 10 FESEM–EDS analyses of one couple of the third series prepared with the inverse configuration, i.e. with BFO placed as the inside (and previously cured) pellet. As observed after curing this BFO pellet for just 15 min, no diffusion of Ti and Fe into the respective BFO and BiT pellets is anymore produced.

structure is formed no iron species can be released to freely diffuse across the interface. As a matter of fact, this last finding shall be considered as an effective strategy to avoid any unwanted diffusion at the composite interface; moreover, it may be particularly useful for a multilayer-type assembly that typically involves the use of highly reactive powders (e.g. sol-gel precipitates): by flash annealing the BFO film prior to the deposition of the BiT layer, no further inter-diffusion processes would be expected between the two nominal components, so eventually the potential multiferroic properties of the system would not be conditioned by any unwanted solid state diffusion process.

Conclusions

The diffusion trends in the nominal $\text{Bi}_4\text{Ti}_3\text{O}_{12}$ – BiFeO_3 composite system have been analysed as a function of the specific reactivity of the starting powders configuring the composite. The obtained results indicate that no diffusion is ever produced from the preformed $\text{Bi}_4\text{Ti}_3\text{O}_{12}$ and BiFeO_3 double oxides. Similarly no significant diffusion is observed when dealing with the respective raw oxide precursors, both TiO_2 and Fe_2O_3 exhibiting the same poor inertia to diffuse. However, when starting from a more reactive condition like that of a precipitated powder, although no diffusion of titanium is still detected, a short-range diffusion of iron into the confronted $\text{Bi}_4\text{Ti}_3\text{O}_{12}$ pellet is produced. Certainly, this diffusion could be a serious obstacle for an optimum magnetoelectric coupling at the composite interface and should be taken into account when conceiving/building the specific composite array. For example, in the case of a multilayer configuration our results also demonstrate that a fast annealing of the BiFeO_3 nominal layer before depositing the $\text{Bi}_4\text{Ti}_3\text{O}_{12}$ layer can prevent such movement of iron towards the BiT side, so the potential multiferroic properties of the system would not be conditioned by any unwanted solid state diffusion process.

Acknowledgements

This work was supported by the Spanish Ministry of Economy and Competitiveness, MINECO [Projects MAT2013-40722-R and MAT2014-59210-JIN] and the Spanish Council of Scientific Research, CSIC [Project CSIC 201460E104]. Marco Peiteado also acknowledges the Ramon y Cajal Grant for the financial support.

References

- [1] Spaldin NA, Fiebig M (2005) The renaissance of magnetoelectric multiferroics. *Science* 309:391–392
- [2] Eerenstein W, Mathur ND, Scott JF (2006) Multiferroic and magnetic materials. *Nature* 442:759–765
- [3] Catalan G, Scott JF (2009) Physics and applications of bismuth ferrite. *Adv Mater* 21:2463–2485
- [4] Rong N, Chu M, Tang Y et al (2016) Improved photoelectrocatalytic properties of Ti-doped BiFeO_3 films for water oxidation. *J Mater Sci* 51:5712–5723. doi:10.1007/s10853-016-9873-z
- [5] Bernardo MS, Jardiel T, Peiteado M et al (2013) Intrinsic compositional inhomogeneities in bulk Ti-doped BiFeO_3 : microstructure development and multiferroic properties. *Chem Mater* 25:1533–1541
- [6] Rojas-George G, Concha-Balderrama A, Esparza-Ponce H et al (2016) Local polarization switching in Ba–Ni co-doped BiFeO_3 thin films with low rhombohedral-symmetry distortion. *J Mater Sci* 51:2283–2291. doi:10.1007/s10853-015-9530-y
- [7] Vaz CAF, Hoffman J, Ahn CH et al (2012) Magnetoelectric coupling effects in multiferroic complex oxide composite structures. *Adv Mater* 22:2900–2918
- [8] Martin LW, Ramesh R (2012) Multiferroic and magnetoelectric heterostructures. *Acta Mater* 60:2449–2470
- [9] Adhlakha N, Yadav KL, Singh R (2016) BiFeO_3 – CoFe_2O_4 – PbTiO_3 composites: structural, multiferroic, and optical characteristics. *J Mater Sci* 50:2073–2084. doi:10.1007/s10853-014-8769-z
- [10] Roy S, Majumder SB (2012) Recent advances in multiferroic thin films and composites. *J Alloy Compd* 538:153–159
- [11] Semenov AA, Dedyk AI, Nikitin AA (2016) Artificial multiferroic structures based on barium-strontium titanate. *J Mater Sci* 51:7803–7813. doi:10.1007/s10853-016-0090-6
- [12] Ma J, Hu J, Li Z et al (2011) Recent progress in multiferroic magnetoelectric composites: from bulk to thin films. *Adv Mater* 23:1062–1087
- [13] Vaz CAF (2013) Artificial multiferroic heterostructures. *J Mater Chem C* 1:6731–6742
- [14] De Frutos J, Matutes-Aquino JA, Cebollada F et al (2007) Synthesis and characterization of electroceramics with magnetoelectric properties. *J Eur Ceram Soc* 27:3663–3666
- [15] Andrew JS, Starr JD, Budi MAK (2014) Prospects for nanostructured multiferroic composite materials. *Scr Mater* 74:38–43
- [16] Bernardo MS (2014) Synthesis, microstructure and properties of BiFeO_3 -based multiferroic materials: a review. *Bol Soc Esp Ceram V* 53:1–14
- [17] Jardiel T, Caballero AC, Villegas M (2008) Aurivillius ceramics: $\text{Bi}_4\text{Ti}_3\text{O}_{12}$ -based piezoelectrics. *J Ceram Soc Jpn* 116:511–518
- [18] Jardiel T, Caballero AC, Fernandez JF et al (2006) Domain structure of $\text{Bi}_4\text{Ti}_3\text{O}_{12}$ ceramics revealed by chemical etching. *J Eur Ceram Soc* 26:2823–2826
- [19] Srinivas A, Suryanarayana SV, Kumar GS et al (1999) Magnetoelectric measurements on $\text{Bi}_5\text{FeTi}_3\text{O}_{15}$ and $\text{Bi}_6\text{Fe}_2\text{Ti}_3\text{O}_{18}$. *J Phys-Condens Matter* 11:3335–3340
- [20] Li JB, Huang YP, Rao GH et al (2010) Ferroelectric transition of Aurivillius compounds $\text{Bi}_5\text{FeTi}_3\text{O}_{15}$ and $\text{Bi}_6\text{Fe}_2\text{Ti}_3\text{O}_{18}$. *Appl Phys Lett* 96:222903

- [21] Chen G, Bai W, Sun L et al (2013) Processing optimization and sintering time dependent magnetic and optical behaviors of Aurivillius $\text{Bi}_5\text{Ti}_3\text{FeO}_{15}$ ceramics. *J Appl Phys* 113:034901
- [22] Lomanova NA, Morozov MI, Ugol'kov VL et al (2006) Properties of aurivillius phases in the $\text{Bi}_4\text{Ti}_3\text{O}_{12}$ - BiFeO_3 system. *Inorg Mater* 42:189–195
- [23] Jiang PP, Zhang XL, Chang P et al (2014) Spin-phonon interactions of multiferroic $\text{Bi}_4\text{Ti}_3\text{O}_{12}$ - BiFeO_3 ceramics: low-temperature Raman scattering and infrared reflectance spectra investigations. *J Appl Phys* 115:144101
- [24] Yi SW, Kim SS, Kim JW et al (2009) Multiferroic properties of $\text{BiFeO}_3/\text{Bi}_4\text{Ti}_3\text{O}_{12}$ double-layered thin films fabricated by chemical solution deposition. *Thin Solid Films* 517:6737–6741
- [25] Zhou J, Wu FX, Chen YB (2012) Structural stability of layered n- LaFeO_3 - $\text{Bi}_4\text{Ti}_3\text{O}_{12}$, BiFeO_3 - $\text{Bi}_4\text{Ti}_3\text{O}_{12}$, and SrTiO_3 - $\text{Bi}_4\text{Ti}_3\text{O}_{12}$ thin films. *J Mater Res* 27:2956–2964
- [26] Makovec D, Kolar D, Trontelj M (1993) Sintering and microstructural development of metal oxide varistor ceramics. *Mater Res Bull* 28:803–811
- [27] Peiteado M, Makovec D, Villegas M et al (2008) Influence of crystal structure on the Co-II diffusion behavior in the $\text{Zn}_{1-x}\text{Co}_x\text{O}$ system. *J Solid State Chem* 181:2456–2461
- [28] Bernardo MS, Jardiel T, Peiteado M et al (2011) Reaction pathways in the solid state synthesis of multiferroic BiFeO_3 . *J Eur Ceram Soc* 31:3047–3053
- [29] Xu H, Du Y, Zhou Y et al (2006) Determination of phase diagrams using the diffusion couple technique. *Rare Met* 25:427–430
- [30] Wang J, Zhang YN, Hudon P (2015) Experimental determination of the phase equilibria in the Mg–Zn–Sr ternary system. *J Mater Sci* 50:7636–7646. doi:10.1007/s10853-015-9326-0
- [31] Bernardo MS, Jardiel T, Peiteado M et al (2011) Sintering and microstructural characterization of W^{6+} , Nb^{5+} and Ti^{4+} iron-substituted BiFeO_3 . *J Alloy Compd* 509:7290–7296
- [32] Jardiel T, Caballero AC, Villegas M (2006) Sintering kinetic of $\text{Bi}_4\text{Ti}_3\text{O}_{12}$ based ceramics. *Bol Soc Esp Ceram V* 45:202–206
- [33] Peiteado M, Caballero AC, Makovec D (2007) Diffusion and reactivity of ZnO-MnO_x system. *J Solid State Chem* 180:2459–2464
- [34] Rahaman MN (2003) *Ceramics processing and sintering*, 2nd edn. Marcel Dekker Inc., New York, pp 336–357